

1st Year Lab Reflective Statement: Cycle 2 Lab Report

Self-Reflection is an important part of learning, it can help you to develop your skills and review their effectiveness, rather than just carrying on doing things as you have always done them.

In this cycle we would like you to reflect on the feedback you received for your cycle 1 lab report. Please copy the feedback summary you received into box 1 and use box 2 to briefly describe what you have done to address that feedback in your cycle 2 lab report. The reflective statement does not contribute to your grade.

When you have finished, please add this sheet as a cover page to your lab report and submit the combined document as a single PDF.

1. Feedback Summary from Cycle 1 lab report:

2. How have you responded to the feedback you received in cycle 1?

- Very good effort. The general structure and contents are satisfactory.

- The general organisation and the style of the report are very inconsistent. Try to keep the fonts the same size, colour and style throughout the report.

- Fonts in report are all in Times New Roman instead of LaTeX font as previously used. There is consistency among the fonts in the main body, and among captions.
- Remove unnecessary highlighting, different fonts, dropcaps was deemed too “fancy”.
- The font size of the references is now increased to the same scaling as previously mentioned (last time I didn’t realise that the references didn’t count towards the page limit!)
- Figure captions are now consistently below each respective figure as mentioned.
- Irrelevant code snippets removed. Instead mentioned briefly in the Appendix.
- More spacing added between sections.

- Refer to other peer-reviewed scientific publications for what the standard format is. (Avoid any 'fancy' styling since they are not really necessary).

- Removal of dropcaps and the use of different fonts to refer to code.
- IEEE referencing used throughout references section
- Removal of hyperlinks from referencing, and far fewer references from websites.
- Included date of lab report submission in byline.

- Figures need to be of better quality in general with appropriate sizing.

- Removal of photographic diagrams of experimental set-up.
- All diagrams are now schematic representations with at least 500dpi.
- No more hand-drawn figures, instead created using digital software.
- Figures are scaled as large as column margins permit.
- Attempted to increase text clarity in figures where possible.

Measuring the Rydberg Constant with a Diffraction Grating

Martin He, Student at Imperial College London, Blackett Laboratory

17th February 2022

ABSTRACT --- We can ascertain the value of the Rydberg constant to a degree of accuracy of approximately 0.4%^[1], through the use of a spectrometer. This was done by initially determining the diffraction angles of different hydrogen emission spectral lines which had passed through a diffraction grating of approximately 78.8 lines per mm. With the angles we obtained, we linearly related these angular displacements to the maxima order numbers (n) of three different colours observed in the Balmer series. From the subsequent plots for each of the three exhibited wavelengths, the Rydberg constant was determined to have a value of $(1.093 \pm 0.005) \times 10^7 \text{ m}^{-1}$.

I. INTRODUCTION

This experiment attempts to obtain a value for the Rydberg constant (R_H) through the analysis of the diffraction angles of the maxima for various wavelengths of light found in the Balmer series, from which its value can be obtained. Our experimental setup was comprised of three main components: a hydrogen lamp, a diffraction grating mounted onto a spectrometer table, and a telescope. The constant is of considerable importance in atomic physics due to the high degree of precision^[2] at which it can be calculated, coupled with its relation with several fundamental constants^[3] in Physics, namely c , h , e , m_e , and ϵ_0 , allowing for the quick calculation of characteristic frequencies in emission spectra. Additionally, it is of historical significance in the development of quantum mechanics: as part of the Bohr model, it makes an excellent approximation of the hydrogen spectral series^[4] through its inclusion in the Rydberg formula, and allows for the precision testing for QED^[5] (as correct to 1 in 10^8). It also has far-ranging applications, such as in Chemistry, where it is used to relate the energy of each orbital^[6], E_n , to the inverse square of its principal quantum number. This is then used in conjunction with the orbital angular momentum quantum number, l , that are ascribed letters such as: 's', 'p', 'd', 'f', 'g', (e.g. as part of the *Aufbau principle*), extending beyond hydrogen-like atoms to form the basis of MO theory^[7].

II. THEORY

The description of electron transitions in hydrogen atoms is founded upon the Bohr atomic model, where Rydberg initially built upon the empirical observations^[8] made by Balmer; we can also link the behaviour of light travelling through a diffraction grating to its wave-like properties. If we consider an idealised set-up with infinitesimally narrow slits at a large distance away from the observer (such that the rays are assumed parallel^[9]), concerning the path difference of light passing through a diffraction grating with N equally-spaced narrow slits, we have:

$$\text{path difference} \cdot \frac{2\pi}{\lambda} = 2\pi n \Rightarrow d \sin \theta \cdot \frac{2\pi}{\lambda} = 2\pi n \quad (1)$$

which gives the formula for phase difference, where d gives the spacing of the slits, n is the maxima order number, λ is the wavelength of light, and the path difference is given by $d \cdot \sin \theta$.

Consequently:

$$d \sin \theta = n \lambda \quad (2)$$

From this equation, we can relate the wavelength of light in the Balmer series with n and θ from the central maximum as shown in **Figures 2, 3** and **4**. For a plot of $\sin \theta$ against n , each wavelength is therefore given by the gradient divided by d . The Rydberg formula for hydrogen^[10] is given by:

$$\frac{1}{\lambda} = -R_H \left(\frac{1}{n^2} - \frac{1}{p^2} \right) \quad (3)$$

where n and p give the principal quantum numbers of initial and final energy levels during an electron transition, and λ gives the wavelength of electromagnetic radiation emitted in a vacuum. As a result, the linear plot of the reciprocal of λ against the exact values of $\frac{1}{n^2} - \frac{1}{p^2}$ yield a negatively correlated linear fit, of which the gradient is $-R_H$. It is therefore possible to obtain an experimental value for the Rydberg constant through the interpolation of this data, along with its propagated uncertainty [see Appendix I].

Additionally, the Rydberg constant for hydrogen (R_H) and the fine structure constant (α) are respectively defined as^[11]:

$$R_H = \frac{\alpha^2 m_e c}{2h} \quad \text{where} \quad \alpha = \frac{e^2}{4\pi\epsilon_0 \hbar c} \quad (4)$$

where R_H is defined in terms of the constants: α , m_e , c , and h , and α is in turn defined by e , ϵ_0 and c . Combining and evaluating these two equations, we have that the theoretical value of the Rydberg constant is found to be $10973731.6 \text{ m}^{-1}$.

III. EXPERIMENTAL METHOD

The various parts of the spectrometer which were used during the experiment are labelled below^[12] in **Figure 1**, with their uses outlined in *brackets* below throughout the method:

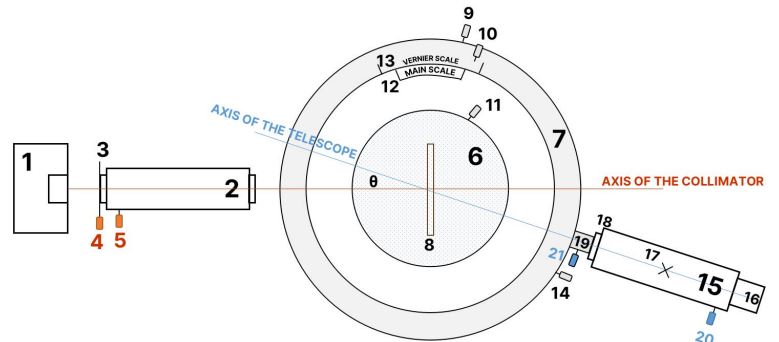


FIGURE 1: Schematic diagram (*bird's eye view*) of the spectrometer used during the experiment, prior to alignment. *Labels:* 1 - Hydrogen Lamp (or Sodium for the calibration process), 2 - Collimator, consisting of: (3) slit plate, (4) slit width adjustment screw, (5) focus knob. 6 - Spectrometer Table, consisting of: (7) spectrometer table base, (8) diffraction grating with mounting clamp, (9) table rotation, (10) vernier fine adjust lock-screw, (11) spectrometer table rotation/height adjust lever, (12) main scale, (13) vernier scale, (14) table rotation lock-screw. 15 - Telescope, consisting of: (16) eyepiece, with graticule lock-ring, (17) cross-hair, (18) camera lens, (19) telescope base, (20) focus knob, (21) telescope fine rotation knob.

A telescope was focused onto a distant object,^[12] by adjusting the focus knob (20), and then rotated it so that it was in line with the axis of the collimator (*shown in orange*). A sodium lamp, initially, was turned on and positioned near the slit (3), and the slit width screw (4) adjusted until an image of the slit on the cross-hair (17) was in sharp focus,^[12] with its angular position recorded using the main (12) and vernier scales (13) for reference. Following this, we rotated the lens tube, so that the cross-hair was in the shape of an “x”. The telescope was moved precisely through 90° and clamped in place, taking note of the new reading, such that the axes of the telescope and collimator were now perpendicular. Next, we rotated the grating table (8) until a reflected image of the slit was observed at the eyepiece, indicating that the mirror surface was 45° to the incident beam from the collimator. The height of the image was adjusted, using adjustment screws (11) found under the grating table to realign the centre of the slit. We then swapped the sodium lamp, which was used during the calibration, for the hydrogen lamp - doing so prevented the hydrogen lamp from burning out when its use wasn't required.

Preliminary observations compared the use of an 80 lines per mm and 300 lines per mm diffraction grating respectively, with the former being selected due to an increased number of maxima observed across different wavelengths of light seen in the Balmer series. It was ensured that the grating rulings were aligned with the telescope's rotational axis, by rotating through large angles and ensuring the image was in line with the cross-hair (17), so that the recorded values of θ were along the axis of rotation. We then proceeded to measure the range of values over which maxima were observed, finding these, in general, to vary over ± 3 arc-minutes on either side. The hydrogen lamp was switched off between readings.

The angles through which the central maximum occurred were noted using the main (in increments of $\pm \frac{1}{2}^\circ$) and vernier scales (in increments of $\pm \frac{1}{60}^\circ$). This was subsequently repeated for the remainder of the maxima, for which their scale readings were digitally captured from a fixed position and later verified for the sake of reducing ambiguity in the collection of readings in the dark, as well as reducing subjectivity and potential parallax errors in reading the scale.

IV. ERRORS, RESULTS AND DISCUSSION

Maxima from three distinct wavelengths of light in the Balmer series were observed, which were found to correspond to the transitions^[13] from $n = 3, 4$, and 5 , the colours we refer to as ‘red’, ‘cyan’, and ‘violet’ respectively. We recorded at least a dozen maxima for each, which were generally distributed symmetrically about the central maxima. The results are displayed in **Figures 2, 3** and **4**. On account of the diffraction grating employing an older definition of 2001 lines per inch, as per the manufacturer^[13], the number of lines per unit length approximates to roughly 78.8 lines per mm instead of the quoted 80 lines per mm. Without this correction, there would be a systematic shift upwards in **Figure 5** which would've otherwise resulted in a calculated value of $R_H = 1.11 \times 10^7 \text{ m}^{-1}$.

The following linear fits result from a least-square regression. We calculated the sine of the angles at the upper and lower end of each uncertainty range of each maxima, taking the difference from the sine of the mean, leading to unequal error bars. These uncertainties, which were treated in an absolute sense, were incorporated into each fitting [see Appendix I].

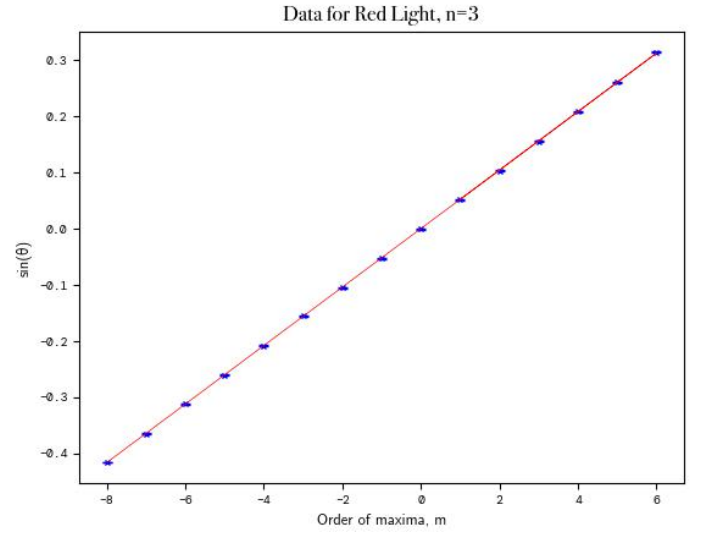


FIGURE 2: Linear plot of $\sin(\theta)$, where θ represents the angle of displacement from the central maxima, against order number of the maxima (m), for $n = 3$ in the Balmer series. All data points are intercepted by the line of best fit. *N.B:* the error bars included in the graph are vertical. As the maxima order numbers are discrete, consequently, no uncertainty can be attributed to these integer values.

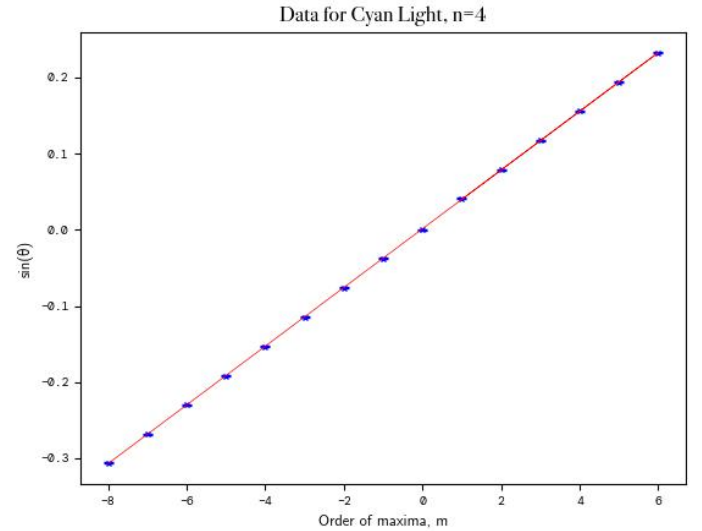


FIGURE 3: The linear plot for $n = 4$ in the Balmer series. All data points are intercepted by the line of best fit. A greater number of maxima were observed in $n=4$ than for the $n=3$ data, as the cyan colour was clearer to observe.

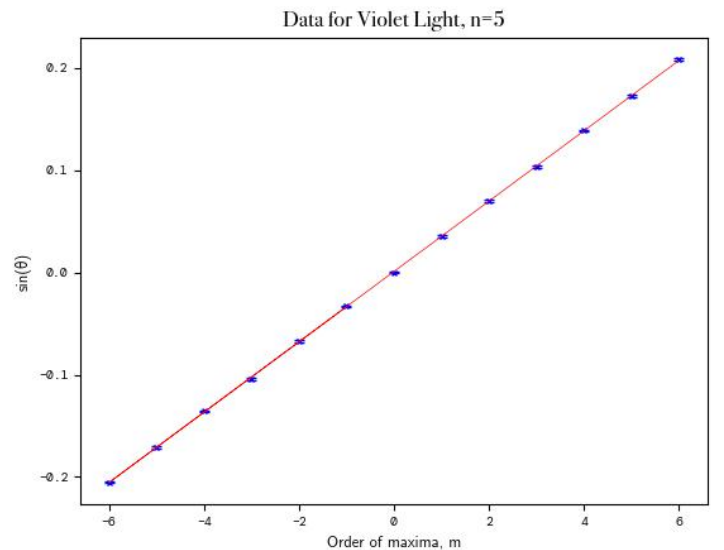


FIGURE 4: The linear plot for $n = 5$ in the Balmer series. All data points are intercepted by the line of best fit. Due to the increasing faintness of subsequent maxima beyond $m=\pm 6$, no further readings were taken. The $n = 5$ transition colour is commonly known as “blue”, but we agreed it looked more violet so it is referred to as such throughout this report.

From **Figures 2 to 4**, we obtained the following values of λ which deviate by 0.41%, 0.35%, and 0.41% respectively from the established wavelengths^[14] found in the Balmer series. These values are presented in **Table 1**.

n	COLOUR	$\lambda_{\text{observed}} / \text{nm}$	$\lambda_{\text{actual}} / \text{nm}$
3	RED	659.0 ± 0.6	656.3
4	CYAN	487.9 ± 0.6	486.2
5	VIOLET	435.9 ± 0.8	434.1

TABLE 1: A comparison of established wavelengths in the Balmer series against data obtained from the experiment. Uncertainty ranges for the gradient of the linear fit, and by extension, the obtained value for the wavelength, incorporated both the uncertainty in the diffraction grating slit spacing, as well as the uncertainties determined in each value. Whilst wavelengths lie outside of the determined absolute uncertainty ranges, they all remain accurate to within 0.5% of their true values.

Performing χ^2 tests on each of the best fit lines in **Figures 2 to 4**, we obtain the values 0.001, 0.003, and 0.004 respectively, whilst a final χ^2 test on **Figure 5**, which has two degrees of freedom, resulted in the value of 0.50: none of which were statistically significant. Consequently, there is insufficient evidence to suggest that any of the linear fits were poor at the 5% significance level (such as, in Fig. 5, $\chi^2_2 = 5.991 \gg 0.50$). Performing a Pearson correlation test on each of the following as before yields the following coefficients $\rho = 0.999995$, 0.999992, and 0.99997, with a final value of $\rho = -0.999998$, suggesting strong linear correlations throughout.

Using Eq. 3, and the data in **Figures 2 to 4**, **Figure 5** was plotted from which we can determine our value of R_H :

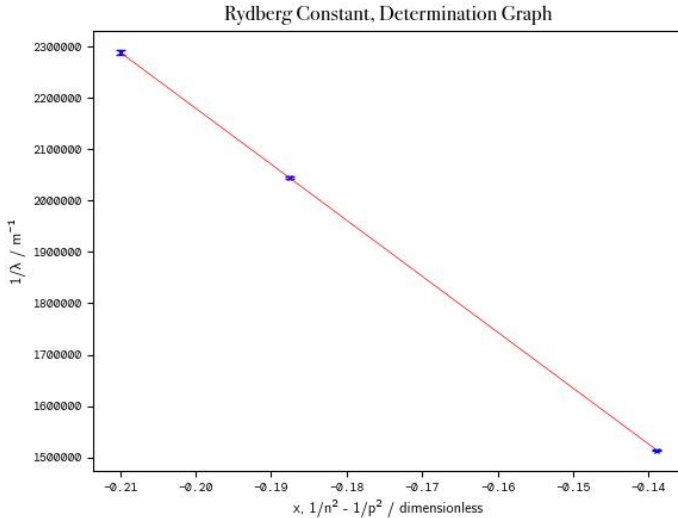


FIGURE 5: Linear plot of $\frac{1}{\lambda}$, referred to here by the dimensionless constant x , where n and p represent the initial, and final energy levels of a hydrogen orbital electron respectively, against $\frac{1}{\lambda}$.

Thus, this value was found to be $(1.0931 \pm 0.0048) \times 10^7 \text{ m}^{-1}$, yielding an absolute uncertainty of 0.44%. We previously found the theoretical value for R_H to be $10973731.6 \text{ m}^{-1}$ ^[15], which differs by 0.39% from our experimental value. This corresponds to being within 89% of our uncertainty range.

One major source of error likely to have arisen during this experiment arose from misalignment of the spectrometer with the grating, which was judged to be perpendicular to the beam of light by eye. As well as this, the determination of the location of each maxima relied on a degree of judgement which hindered the precision of our results, whilst temperature, air humidity, and ambient lighting were minor contributions^[16] to the uncertainty which were unquantified.

V. CONCLUSION

We have outlined a method for the determination of the Rydberg constant using a spectrometer. This relied upon the measurement of the angular dispersions of spectral lines after they had passed through a diffraction grating, resulting in a value of $(1.093 \pm 0.005) \times 10^7 \text{ m}^{-1}$: the accepted value lies within our calculated uncertainty range.

In order to address several shortcomings of this experiment, we propose the following experimental method. As before, the spectrometer is set up, however, with a CMOS camera aligned level at the eyepiece lens. As part of the alignment of the grating, a horizontal line can be superimposed on the camera view (e.g. using the ThorCam™ application^[17]), as minute adjustments are made with the adjustment screws to result in perfect alignment. Looking directly onwards into the eyepiece lens, a multichromatic CMOS camera, set to low exposure time to prevent image oversaturation, would capture several photos, noting the angular readings. Thus, by ascertaining the field of vision of the camera and what angular readings these corresponds to (using the crosshair), images can be digitally ‘stitched’ together along an angular profile. By performing a series of Fourier Transforms^[18], we can also resolve the image and overlapping maxima, by applying masks (of which we can determine its component colours) to the split RGB channels. With the resultant masked images for each λ , an objective analysis of the intensity profiles, as processed in ImageJ^[19] or OpenCV, can be performed, thus determining the central point in each maxima, with the attributed uncertainty originating from the resolution of the vernier scale ($\pm \frac{1}{60}^\circ$).

Background lighting would be further reduced, switched on and off between readings and image captures. Further investigation into the use of diffraction gratings with differing slit separations would also be conducted. Whilst finer gratings result in more concentrated patterns (thus a larger number of observed maxima,) there is an increase in the uncertainty in the position of each. With a sufficiently high-res CMOS camera, however, the impacts of this would be mitigated. Thus, the value of R_H , for gratings of various slit widths, can be compared in a standardised manner. The reliance on the Bohr model of the atom, however, means that its value cannot be ascertained solely from frequencies in hydrogen alone, but requires deuterium and antiprotonic helium as well, using the frameworks of QED^[20] to account for effects such as hyperfine splitting and fine structure^[21] for extreme precision.

VI. REFERENCES AND APPENDICES

Appendix I - Error Propagation in the Data Analysis, and the Incorporation of Error in Subsequent Linear Fits

The use of *numpy*’s polyfit function does not allow for the uncertainty in each value to be taken into account of, nor is this incorporated into the resultant covariance matrix of parameters. An improved method employs the use of *scipy*’s curve_fit function allowing both via use of a *sigma* parameter, with *absolute_sigma* set to True. This, in effect, calculates the maximum and minimum lines of best fit for each of **Figures 2, 3, and 4**, translating this to the value of gradient they correspond to, and their deviation from the optimal linear fitting. Following this, the *uncertainties* package^[22] was utilised to efficiently calculate propagated error. The results of which were then in turn incorporated into the subsequent linear fitting in **Figure 5**. Consequently, the final experimental value of the Rydberg constant, which is calculable from the gradient, incorporated all of its component uncertainties, as part of its covariance matrix of parameters, which results in the value of $\pm 0.048 \text{ m}^{-1}$. The source code can be found at the following [Github repository](#).

REFERENCES

- [1] NIST, 2018. Fundamental Physical Constants. CODATA Value: Rydberg Constant. from National Institute of Standards and Tech. Available at: <https://physics.nist.gov/cgi-bin/cuu/Value?ryd> [Online][Accessed January 25, 2022].
- [2] Pohl, R., Antognini, A., Nez, F. et al. The size of the proton. *Nature* 466, 213–216 (2010). <https://doi.org/10.1038/nature09250>
- [3] ‘S. P. D. Mangles et. al (Ed.) ‘Year 1 Laboratory Manual: Diffraction Experiments’, Imperial College London, 2020-21, pp. 3 [Accessed January 20, 2022]
- [4] Ling, S., Sanny, J. and Moebs, W., 2021. University Physics Vol. 3. Rice University, pp.269-272.
- [5] P. Cladé et al., "Determination of the Fine Structure Constant Based on Bloch Oscillations of Ultracold Atoms in a Vertical Optical Lattice", *Physical Review Letters*, vol. 96, no. 3, 2006. Available: 10.1103/physrevlett.96.033001.
- [6] Keeler, J. & Wothers, P., 2009. *Why Chemical Reactions Happen* 5th ed., Oxford, United Kingdom: Oxford University Press. pp. 43-47, pp. 51-57
- [7] Keeler, J. & Wothers, P., 2009. *Why Chemical Reactions Happen* 5th ed., Oxford, United Kingdom: Oxford University Press. pp. 62-65, pp.68-69
- [8] J. Rydberg, ‘Researches sur la constitution des spectres d’émission des éléments chimiques’, Kongliga Svenska Vetenskaps-Akademien Handlingar, University of Michigan, pp.253
- [9] R. Feynman, R. Leighton and M. Sands, *Feynman Lectures on Physics*, 3rd ed. New York: Basic Books, 2015, Ch. 30-2.
- [10] ‘S. P. D. Mangles et. al (Ed.) ‘Year 1 Laboratory Manual: Diffraction Experiments’, Imperial College London, 2020-21, pp. 5 [Accessed February 16, 2022]
- [11] Ling, S., Sanny, J. and Moebs, W., 2021. University Physics Vol. 3. Rice University, pp.269-272.
- [12] PASCO SP-9268A Student Spectrometer User Manual, PASCO, <https://www.pasco.com/products/lab-apparatus/light-and-optics/spectrometers/sp-9268>, pp.2-3 [Online][Accessed February 16, 2022]
- [13] ‘S. P. D. Mangles et. al (Ed.) ‘Year 1 Laboratory Manual: Diffraction Experiments’, Imperial College London, 2020-21, pp. 6 [Accessed January 20, 2022]
- [14] Suplee et. al, NIST, 2021. Atomic Spectra Database. Available at: <https://www.nist.gov/pml/atomic-spectra-database> [Online] [Accessed January 25, 2022].
- [15] NIST, 2018, Fundamental Physical Constants from NIST. Available at: <http://physics.nist.gov/constants> [Online] [Accessed January 25, 2022].
- [16] ‘S. P. D. Mangles et. al (Ed.) ‘Year 1 Laboratory Manual: Diffraction Experiments’, Imperial College London, 2020-21, pp. 5-6 [Accessed January 20, 2022]
- [17] ThorLabs, ThorCam™ Application User Manual, Available at: <https://seltokphotonics.com/upload/iblock/0c5/0c51400dfad8626e93ae5d9e1f3ecbf0.pdf> [Online] [Accessed: January 25, 2022]
- [18] An example of how this method could be applied along with its processed result using sample generated data can be found at the following [Github repository](#). Requires OpenCV library, and ImageJ. The subsequent images, processed using the Horizontal Intensity Profile Tool in ImageJ to output a CSV file, can then be analysed using analysis.py to determine the central position of each maxima.
- [19] ImageJ. 2012. Image J User Guide. pp. 6 [online] Available at: <<https://imagej.nih.gov/ij/docs/guide/user-guide.pdf>> [Online] [Accessed February, 16 2022].
- [20] Karshenboim, S., 2008. New Recommended Values of the Fundamental Physical Constants (CODATA 2006). *Physics-Uspekhi*, 51(10), pp.639-651.
- [21] Akhiezer, A. and Berestetskii, V., 1965. *Quantum Electrodynamics*. New York: Interscience.
- [22] Lebigot, "Welcome to the Uncertainties Package — uncertainties Python package 3.0.3 documentation", 2022. Available: <https://uncertainties-python-package.readthedocs.io/en/latest/>. [Online] [Accessed: January 25, 2022]

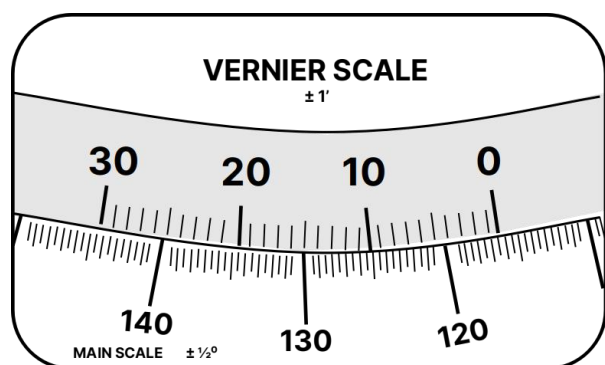


FIGURE 6: Schematic of Vernier (*top*) and Main (*bottom*) Scales on the Spectrometer. Adapted from: PASCO SP-9268 User Manual.

- [13] ‘S. P. D. Mangles et. al (Ed.) ‘Year 1 Laboratory Manual: Diffraction Experiments’, Imperial College London, 2020-21, pp. 6 [Accessed January 20, 2022]
- [14] Suplee et. al, NIST, 2021. Atomic Spectra Database. Available at: <https://www.nist.gov/pml/atomic-spectra-database> [Online] [Accessed January 25, 2022].